Infection and Immunity

In Vivo Physiological and Transcriptional Profiling Reveals Host Responses to Clostridium difficile Toxin A and Toxin B

Kevin M. D'Auria, Glynis L. Kolling, Gina M. Donato, Cirle A. Warren, Mary C. Gray, Erik L. Hewlett and Jason A. Papin
Infect. Immun. **2013, 81(10):3814. DOI: 10.1128/IAI.00869-13. Published Ahead of Print 29 July 2013.**

IAI Journals.ASM.org

In Vivo Physiological and Transcriptional Profiling Reveals Host Responses to *Clostridium difficile* Toxin A and Toxin B

Kevin M. D'Auria,[a] Glynis L. Kolling,[b] Gina M. Donato,[b] Cirle A. Warren,[b] Mary C. Gray,[b] Erik L. Hewlett,[b] Jason A. Papin[a]

Department of Biomedical Engineering[a] and Department of Medicine,[b] Division of Infectious Diseases and International Health, University of Virginia, Charlottesville, Virginia, USA

Toxin A (TcdA) and toxin B (TcdB) of *Clostridium difficile* cause gross pathological changes (e.g., inflammation, secretion, and diarrhea) in the infected host, yet the molecular and cellular pathways leading to observed host responses are poorly understood. To address this gap, we evaluated the effects of single doses of TcdA and/or TcdB injected into the ceca of mice, and several endpoints were analyzed, including tissue pathology, neutrophil infiltration, epithelial-layer gene expression, chemokine levels, and blood cell counts, 2, 6, and 16 h after injection. In addition to confirming TcdA's gross pathological effects, we found that both TcdA and TcdB resulted in neutrophil infiltration. Bioinformatics analyses identified altered expression of genes associated with the metabolism of lipids, fatty acids, and detoxification; small GTPase activity; and immune function and inflammation. Further analysis revealed transient expression of several chemokines (e.g., *Cxcl1* and *Cxcl2*). Antibody neutralization of CXCL1 and CXCL2 did not affect TcdA-induced local pathology or neutrophil infiltration, but it did decrease the peripheral blood neutrophil count. Additionally, low serum levels of CXCL1 and CXCL2 corresponded with greater survival. Although TcdA induced more pronounced transcriptional changes than TcdB and the upregulated chemokine expression was unique to TcdA, the overall transcriptional responses to TcdA and TcdB were strongly correlated, supporting differences primarily in timing and potency rather than differences in the type of intracellular host response. In addition, the transcriptional data revealed novel toxin effects (e.g., altered expression of GTPase-associated and metabolic genes) underlying observed physiological responses to *C. difficile* toxins.

The toxins TcdA and TcdB are two key virulence factors of *Clostridium difficile*, an intestinal, opportunistic pathogen responsible for more than 300,000 infections in the United States per year (2009 data), with several estimates of annual cost between $433 million and $8.2 billion (1–4). Clinical manifestations include leukocytosis and diarrhea. The importance of TcdA and TcdB is underlined by the facts that strains without either toxin colonize but do not cause disease and that intoxication causes manifestations similar to those of infection (5–7). TcdA and TcdB are similar in size, amino acid sequence, and enzymatic specificity yet exhibit different enzymatic activities and *in vivo* potencies (8–10). Furthermore, much remains unknown about common and divergent cellular pathways leading to toxin-mediated host responses (11, 12).

Determining the relative roles of TcdA and TcdB in pathogenesis has proven difficult in part because of variable findings within and between animal models as well as species-specific responses. Clinically, strains lacking TcdA are commonly isolated from infected patients, and no $TcdA^+/TcdB^-$ clinical strain has ever been reported (13). Toxin effects in the context of infection have typically been studied using animal models in which an antibiotic regimen and subsequent disruption of intestinal flora must precede infection with *C. difficile* (14, 15). By generating mutant strains, Lyras et al. found that TcdB but not TcdA was essential for hamster infection, yet Kuehne et al. found, in a similar hamster infection model, that either toxin was sufficient (5, 6). Investigating toxin effects more directly, multiple intoxication models have demonstrated TcdA to be enterotoxic, while TcdB caused little to no pathology (7, 10, 16). However, epithelial damage in human xenografts in mice is greater with TcdB than TcdA, suggesting that many differences in toxin effects are species specific (17). The ability of either toxin to bind, enter, and/or activate intestinal cells may also explain differential effects of TcdA and TcdB. The sequences differ most in the C-terminal binding domain. TcdB has been shown to be incapable of binding the brush border membranes of hamsters, although TcdB has been found to further damage bruised ceca, synergize with TcdA, and contribute to pathogenesis during infection (5, 16, 18). Multiple receptors for TcdA have been proposed or identified, yet the roles of these receptors in different organisms, animal models, and cell types are unclear (19–24). TcdB weakly binds various trisaccharides and oligosaccharides, yet no functional receptor for TcdB has been identified (25). It is also possible that differences in intracellular actions of TcdA versus TcdB are responsible for differences in the host response. Although a similar dose of TcdA or TcdB may result in different gross pathologies, it is unclear if entirely different pathways are activated or repressed or if the same overall functions are affected to different degrees. We previously analyzed the transcriptional response of a human, ileocecal, epithelial cell line

Received 15 July 2013 **Returned for modification** 18 July 2013
Accepted 22 July 2013

Published ahead of print 29 July 2013

Editor: S. R. Blanke

Address correspondence to Erik L. Hewlett, eh2v@virginia.edu, or Jason A. Papin, papin@virginia.edu.

K.M.D. and G.L.K. contributed equally to this work.

E.L.H. and J.A.P. contributed equally to this work.

Supplemental material for this article may be found at http://dx.doi.org/10.1128/IAI.00869-13.

doi:10.1128/IAI.00869-13

(HCT8) to TcdA and TcdB and showed that the toxins induce very similar transcriptional signatures, yet the effects of TcdB occurred earlier (26). In addition, we found altered regulation of many genes involved in cell growth and division but no overwhelming expression of inflammatory markers or other genes associated with physiological changes *in vivo*. The *in vivo* effects of these toxins have not been investigated by measuring genome-wide responses, and many of the links between cellular responses and physiological changes remain unknown. Therefore, we used an *in vivo* system, intracecal injection of toxin into mice, and collected samples to characterize the genome-wide cellular responses and gross physiological effects of each toxin over a 16-h time course.

It has been difficult to tease apart the aspects of the host response to TcdA and TcdB because of the important interactions among the many tissues, cell types, and signals involved (27, 28). The intestinal epithelium, the initial barrier to these toxins, continuously interacts with surrounding cells throughout the development and resolution of disease. Therefore, we focused on the transcriptional response of epithelial-layer cells to toxin and other toxin-related effects. Given the importance of surrounding tissues and with recent evidence of systemic dissemination of toxins, we chose cecal injection of toxin, an open system, as opposed to closed ileal loop models or *ex vivo* systems that may restrict toxin to a limited area (29). Additionally, previous studies have focused on separate facets of the host response, typically with only one toxin per study (30–36). To address these deficits in the knowledge of this illness, we measured genome-wide expression from epithelial-layer cells exposed to TcdA and TcdB to simultaneously capture effects of each toxin.

Using this approach, we identify several genes differentially expressed after toxin treatment that serve as specific candidates to investigate further. Additionally, we employ currently available bioinformatic methods and also introduce novel methods to identify groups of regulated genes associated with known biological functions. Our measurements were taken on several biological levels to link changes in one set of variables (e.g., gene expression) to changes in others (e.g., pathology and blood counts). These linkages serve as tools to validate previous findings as well as identify novel functions affected by TcdA or TcdB. Of the many linkages that could be explored, we further investigated chemokine expression and the role of two chemokines in the response to TcdA cecal injection with respect to changes in pathology, neutrophil recruitment, and survival. In addition to the comparison between toxins and identification of differentially expressed genes, these associations and concepts serve as a basis for further probing the host response to these toxins in the context of *C. difficile* infection.

MATERIALS AND METHODS

Cecal injection. All procedures involving animals were conducted in accordance with the guidelines of the University of Virginia IACUC (protocol no. 3626). Purified TcdA and TcdB were generously provided by David Lyerly at TECHLAB, Inc. Mice (male C57BL/6J, 8 weeks old; Jackson Laboratories) were anesthetized with ketamine-xylazine in preparation for surgery. A midline laparotomy was performed to locate the cecum, and 20 μg of toxin in 100 μl of 0.9% normal saline was injected into the distal tip. Incisions were sutured, and animals were monitored during recovery. Sham-injected animals received only 100 μl of saline. If an animal became moribund (i.e., hunched posture, ruffled coat, or little to no movement), they were immediately euthanized.

Cell culture. An immortalized C57BL/6 mouse cecal epithelial cell line (passage 9) was provided from the laboratory of Eric Houpt and maintained as described by Becker et al. (37). Toxin cytopathicity was assessed by measuring changes in cell adherence and morphology using a multiwell, continuous, electrical impedance assay (xCelligence; ACEA Biosciences). In each well, 20× solutions of TcdA or TcdB (prepared in media) were added 34 h after seeding 21,000 cells, yielding the indicated concentrations.

Blood counts. Blood was collected using cardiac puncture, and complete blood counts were measured using a HEMAVET 950FS (Drew Scientific). Serum was analyzed for levels of systemic chemokines using MILLIPLEX map beads, and the signal was measured using a Luminex 100 IS system (UVA Flow Cytometry Core Facility).

Histology. A cross section from the middle of each cecum was dissected and fixed. The tissues were paraffin-embedded, sectioned, and stained by the UVA histology core. Hematoxylin and eosin (H&E)-stained sections were coded and scored by a blinded observer using parameters to assess inflammation, luminal exudates, mucosa thickening, edema, and epithelial erosions (38). Each of these five parameters was scored between zero and three, yielding total pathology scores between zero and fifteen. Eosinophils were detected in tissue using Congo red staining (39). Tissues for H&E, myeloperoxidase (MPO), and eosinophil staining were fixed in Bouin's solution; tissues for other measurements were fixed in 4% paraformaldehyde. Immunohistochemistry was performed by the Biorepository and Tissue Research Facility at the University of Virginia. Monocytes/macrophages, dendritic cells, and neutrophils were separately identified using the markers F4/80 (clone CI:A3-1; AbD Serotec), Ly75 (EPR5233; Abcam), and MPO (rabbit-anti-MPO; Novus Biologicals), respectively. The presence of neutrophils was quantified by averaging the number of positive cells associated with epithelial and subepithelial layers in 10 random fields (40× objective). Monocyte/macrophage and dendritic cell staining was scored by analyzing each section for the number of positive cells and overall staining intensity. Samples were assigned scores of 1 (few cells/weak staining), 2 (moderate staining), or 3 (many cells/intense staining).

Isolation of cells from cecal tissue. The remaining two sections of each cecum were opened longitudinally, rinsed with Hank's balanced salt solution (HBSS; Gibco), and shaken at 250 rpm for 30 min at 37°C in HBSS containing 50 mM EDTA and 1 mM dithiothreitol (DTT) in order to remove epithelial-layer cells. The digested tissue was strained with a 100-μm cell strainer, and the filtrate was centrifuged (1,000 × *g*, 4°C, 10 min). Cells were resuspended in red-cell lysis buffer (150 mM NH_4Cl, 10 mM $NaHCO_3$, 0.1 mM EDTA) and centrifuged again. The pelleted cells were used immediately for flow cytometry or stored at −80°C until RNA isolation. RNA was isolated using the RNeasy minikit (Qiagen) with on-column DNase digestion according to the manufacturer's instructions. Protein was collected from cell lysate supernatants, which were made using a lysis buffer containing 50 mM HEPES, 1% Triton X-100, and Halt protease inhibitor. The lysate was incubated on ice for 30 min and centrifuged (13,000 × *g*, 4°C, 10 min). Clarified supernatants were stored at −80°C.

Flow cytometry. Epithelial-layer cells were isolated from mice 16 h after injection with TcdA ($n = 2$), TcdB ($n = 3$), or saline control ($n = 3$). The cell preparations were stained with fluorescently conjugated antibodies for several markers, including CD3ε (BV421; BioLegend), cytokeratin (phycoerythrin [PE]; Novus Biologicals), CD11b (allophycocyanin [APC]-Cy7; BioLegend), B220 (fluorescein isothiocyanate [FITC]; BD Bioscience), and CD45 (V500; BD Bioscience) to detect different populations. Samples were analyzed on the CyAn ADP analyzer; 50,000 events were collected and subsequently analyzed using FlowJo software.

Antibody-mediated neutralization of chemokines. For each antibody, 100 μg was administered by intraperitoneal injection 16 h before sham/toxin injection. Mice received a combination of anti-CXCL1 (clone 48415) and anti-CXCL2 (clone 40605) or the relevant isotype controls (clones 54447 and 141945). All antibodies were purchased from R&D

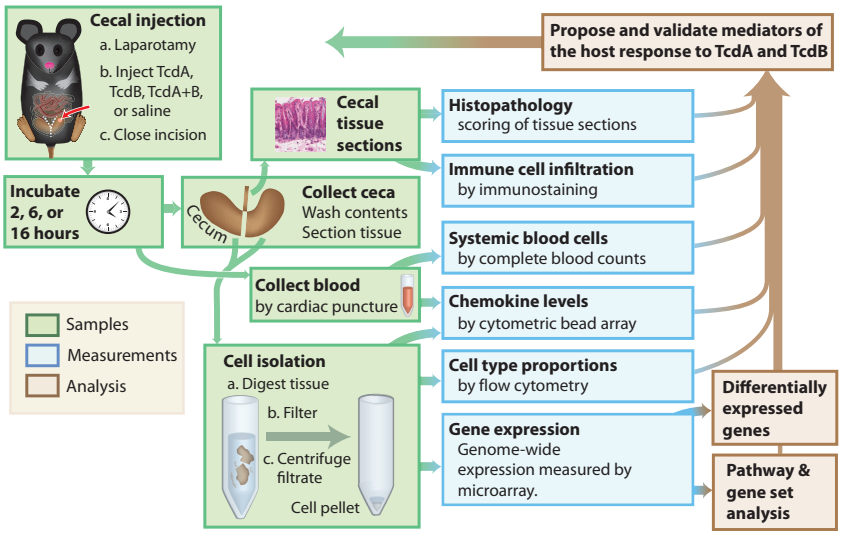

FIG 1 Flow diagram outlining the experimental methods and analyses in this study.

Systems and resuspended according to the manufacturer's directions. Decreased levels of CXCL1 and CXCL2 in the serum of mice receiving neutralizing antibody (compared to isotype controls) indicated that the neutralization was successful.

Microarray procedure. An Agilent 2100 BioAnalyzer was used to assess RNA integrity. cDNA was synthesized, biotin labeled, and hybridized to Affymetrix mouse genome 430 2.0 GeneChip according to the manufacturer's instructions. Arrays were scanned with a GeneChip 3000 7G system (Affymetrix).

Statistical analysis. Unless otherwise stated, each two-sample test is a two-sided Mann-Whitney U test.

Microarray analysis. Full descriptions of the computational and statistical analyses, as well as the data and computer code to reproduce all analyses, figures, and tables, are included in the Supplemental Methods. Briefly, each microarray was background corrected according to the robust multiarray average (RMA) algorithm, and probe sets were summarized using the median polish algorithm (40). All arrays were normalized to each other by cyclic Loess normalization. Differentially expressed genes were detected using the Cyber-T statistical test with a Benjamini-Hochberg *P* value correction (41). Competitive gene set enrichment was performed with a modified version of Wu and Smyth's correlation-adjusted mean rank gene set test (CAMERA) (42). Self-contained gene set enrichment was performed by calculating gene-gene correlations within each gene set.

Additional raw data and computational analyses are available for download (see the supplemental methods in the supplemental material).

Microarray sequence accession number. Microarray data are available from NCBI GEO under data series GSE44091.

RESULTS

Physiological results of toxin cecal injection. TcdA, TcdB, or TcdA and TcdB (TcdA+B) were injected into the cecum to study an anatomical site affected during infection (Fig. 1). The TcdA dose (20 μg/animal) and incubation periods (2, 6, and 16 h) were chosen based on our *in vitro* data and dose-response experiments (see Fig. S1 in the supplemental material) in order to capture the early effects from a single dose of toxin (26). The biological activities of TcdA and TcdB were confirmed using an immortalized mouse cecal epithelial cell line (see Fig. S2 in the supplemental material).

Relative to sham controls, TcdA-challenged mice had greater total pathology scores (more severe pathology) at 2, 6, and 16 h (Fig. 2A and B), with higher scores for all five measured parameters at 16 h ($P < 0.01$), all but mucosa thickening at 6 h ($P < 0.03$), and all but luminal exudates at 2 h ($P < 0.02$). In contrast, the average total pathology score for TcdB-challenged mice was significantly higher than that for sham mice at only 16 h ($P < 0.05$). At 2 h, TcdA+B led to mucosal thickening, inflammation, and edema ($P < 0.04$). Mice challenged with TcdA experienced diarrhea at intermediate and late time points based on visual observations of wet tail and clumped cage bedding. We also examined the colons of mice 16 h after TcdA, TcdB, or sham challenge in order to determine if there are distant effects from the cecal injection. Using the same scoring system, no significant differences in histopathology scores were noted throughout the colon (data not shown).

The complete blood counts and infiltration of immune cells are also altered by TcdA and TcdB. In blood drawn by cardiac puncture 16 h after injection of TcdB, there was an increased concentration of several cell types (see Fig. S3 in the supplemental material). At 16 h, TcdA slightly increased the concentration of monocytes ($P < 0.1$) but decreased the concentrations of lymphocytes and platelets ($P < 0.05$). The increased systemic concentration of monocytes after TcdA challenge is reflected in their infiltration into the cecal submucosa 6 and 16 h after injection (based on immunohistochemistry staining using F4/80; see Table S3 in the supplemental material). In addition, increases in dendritic cells were also evident in the submucosa 6 and 16 h after TcdA challenge. Relative to sham challenge, TcdA and TcdB challenge increased neutrophil infiltration at 16 h ($P \leq 0.02$ using MPO staining), and at 6 h, neutrophil infiltration in four of the six animals challenged with TcdA was greater than neutrophil infiltration in any sham-challenged mouse (Fig. 2C).

Host transcription altered by toxin injection. We evaluated gene expression changes in the epithelial layer to characterize the host cell responses to TcdA and TcdB. To determine the proportions of cell types within our epithelial-layer isolation, we used flow cytometry to analyze cells from mice 16 h after TcdA, TcdB, and sham challenge (see Fig. S4 in the supplemental material). The

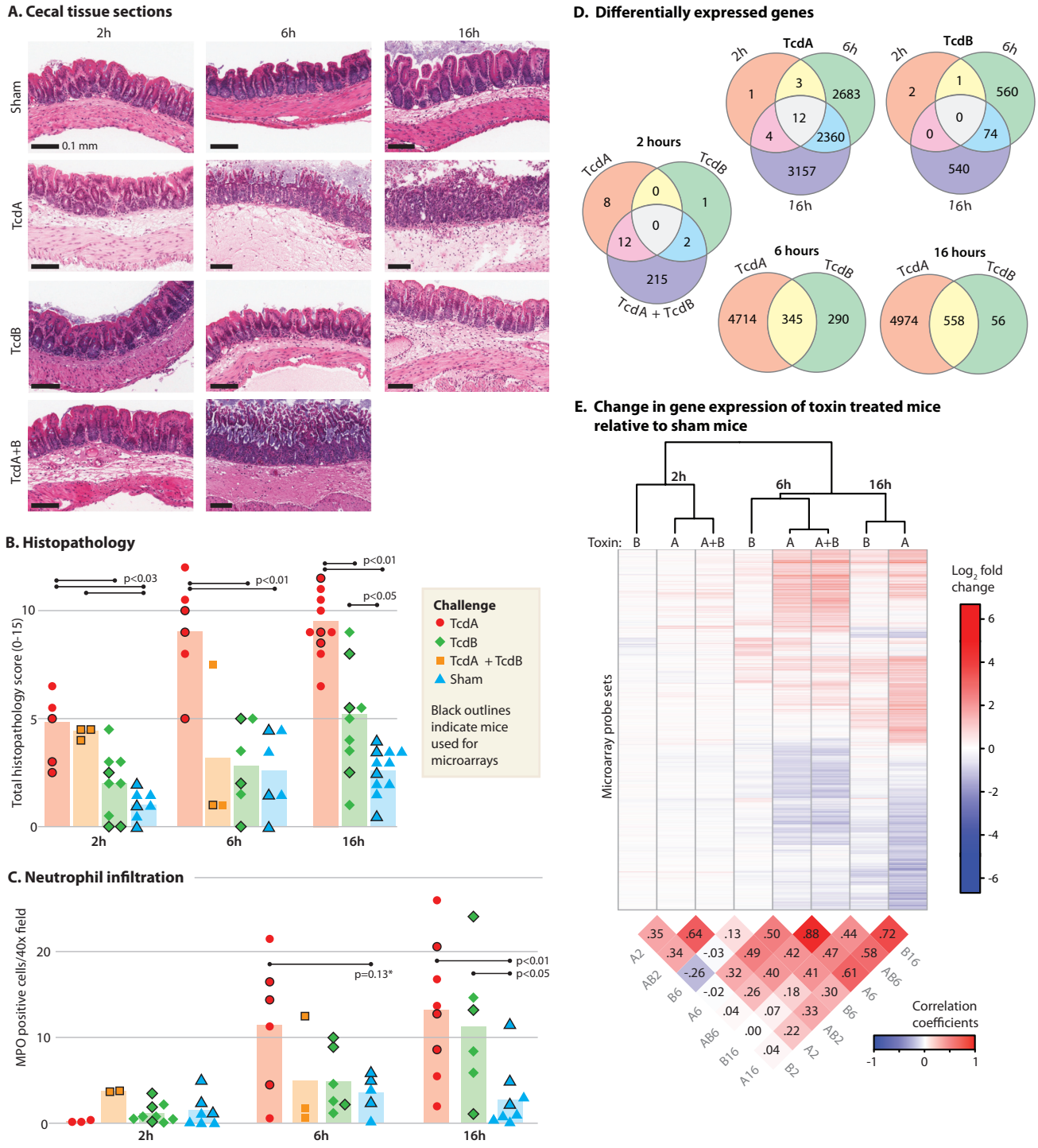

FIG 2 Physiological and gene expression changes after toxin injection. Panels A, B, and C include data combined from four independent experiments with 7, 39, 36, and 12 mice, respectively. In total, 10 of 94 mice did not survive until the experimental endpoint: one TcdA-treated mouse did not survive to 2 h, six mice did not survive to 6 h (1 TcdA, 2 TcdA+B, 1 TcdB, and 2 sham-challenged mice), and six mice did not survive to 16 h (3 TcdB and 3 TcdA mice; see Table S1 in the supplemental material). The data points displayed in the figure were used for each statistical test. The horizontal lines above the bar charts which connect two sample groups indicate a two-sample statistical test. The *P* values for these tests are indicated beside the lines. (A) Representative examples of H&E-stained cecal tissue sections from the 11 indicated sample groups. (B) Total histopathology score (see Materials and Methods) from cecal tissue sections. Except for the two mice injected with TcdA+B (two mice not used for microarrays), histopathology scores were not measured for mice that did not survive. Since two of three mice injected with TcdA+B did not survive to 6 h in our first experiment, we dedicated more mice for TcdA and TcdB at 16 h so that no samples were obtained for TcdA+B at 16 h. All subsequent experiments also excluded the 16-h time point for injection of TcdA+B. (C) The number of cells within the mucosa and immediate submucosa which were positive for MPO after immunohistochemical staining. *, $P = 0.055$ by the two-sided *t* test. (D) Venn diagrams show the overlap of which microarray probe sets are differentially expressed (comparing toxin-challenged mice to sham-challenged mice using a cutoff of $q < 0.01$; see Materials and Methods). All microarray probes are annotated into 45,501 probe sets, each of which represents the expression of one gene or multiple similarly related genes. Since only one microarray was used for TcdA+B at 6 h, statistical tests could not be used to determine differentially expressed genes for that sample group. (E) All probe sets which were differentially expressed for at least one time point were included in the heat map. The Pearson correlation coefficients below the heat map are generated by comparing the log fold changes between each sample group. The dendrogram above the heat map is a hierarchical clustering of the sample groups, using the correlation coefficients as the distance metric.

TABLE 1 Genes with significantly altered expression 2 h after TcdA and TcdB injection

Gene	Fold change[a] in expression after challenge by time point and toxin							
	2 h			6 h			16 h	
	TcdA	TcdB	TcdA+B	TcdA	TcdB	TcdA+B	TcdA	TcdB
Dusp1	4.8	1.3	4.4	6.4	−1.0	10.1	1.9	1.1
Rhob	4.2	1.2	3.8	4.0	1.5	4.8	2.1	1.3
Atf3	4.0	1.4	3.5	2.7	−1.2	4.0	1.2	−2.0
Sprr1a	3.4	1.5	3.7	4.9	−1.1	8.8	−1.6	−1.4
C3	2.8	1.6	1.2	2.2	1.6	3.2	5.7	1.9
Areg	2.6	−1.1	2.5	12.8	2.4	15.5	14.9	5.1
Cxcl10	2.6	2.0	6.8	11.3	1.3	13.3	4.7	2.2
Insig1	2.5	1.5	1.8	−1.9	−1.1	−1.4	−2.3	−1.5
Errfi1	2.5	1.1	2.2	3.4	−1.0	5.5	−1.2	−1.4
Egr1	2.3	−1.1	1.5	2.5	1.9	5.0	3.7	1.4
Zfp36	2.2	1.1	2.0	2.9	1.8	3.4	2.2	1.2
Hmgcs1	1.8	1.2	1.6	−1.2	1.0	−1.1	2.4	1.5
Jun	1.8	1.3	1.6	1.4	1.2	1.6	−1.9	−1.1
Gm11545	1.6	1.1	1.7	7.3	1.9	8.2	5.6	3.8
1700006J14Rik	−1.8	−1.3	−1.2	−1.3	1.4	−1.1	−1.6	−1.1
H3f3b	−2.0	−1.5	−1.3	1.1	2.0	1.4	1.8	1.4
Lrrtm1	−2.3	−2.0	−2.2	−2.3	−1.5	−2.5	−1.9	−1.9
Slc8a1	−2.3	−1.3	−1.7	−3.4	1.4	−2.7	−2.9	1.0
Cxcl1	4.4	2.2	6.5	9.7	1.1	8.1	3.3	1.6
Mtch2	−1.5	−2.0	−1.7	−1.1	2.0	−1.6	−1.5	−1.2
Slc20a1	−1.9	−2.1	−2.5	−2.5	1.7	−2.7	−4.4	−1.5

[a] Average fold changes relative to sham challenge are shown (values of −1.1 and +1.1 imply a 10% decrease and increase, respectively, in gene expression). The cutoff for determining a differentially expressed gene is $q < 0.01$ (see Materials and Methods).

percentage of epithelial cells (cytokeratin$^+$) was similar across all experimental conditions, averaging 85%. Approximately half of the remaining nonepithelial fraction in each experimental condition was leukocytes (CD45$^+$). However, the number of leukocytes was slightly greater for TcdA-challenged mice than sham controls ($P = 0.06$). Within the leukocyte fraction, there was no significant difference between experimental conditions in the percentage of CD3$^+$ cells (average of 40%; T cell marker) or CD11b$^+$ cells (average of 59%; marker for myeloid lineage). However, the percentage of leukocytes positive for B220, a common B cell marker, was greater in TcdB samples than sham samples (60 versus 34%; $P < 0.01$). The remaining nonepithelial fraction, an average of 7.5% of all cells, was not characterized by the markers used. The same epithelial-layer isolation procedure was used for all gene expression measurements.

For both toxins, a small set of genes is affected at 2 h, and at 6 h and 16 h, hundreds or thousands are differentially expressed. A more pronounced TcdA transcriptional response compared to that of TcdB is consistent with TcdA's greater pathophysiological effects *in vivo* (Fig. 2B). However, many of the expression changes induced by TcdA and TcdB are similar. Over 50 and 90% of the genes that are differentially expressed after TcdB treatment at 6 and 16 h, respectively, are also differentially expressed after TcdA treatment (Fig. 2D). Comparing challenge with individual toxins to TcdA+B challenge, the transcriptional response induced by TcdA+B is very similar to that induced by TcdA alone. For instance, at 2 h, 12 of the 20 genes with a significant change in expression after TcdA challenge were also differentially expressed after TcdA+B challenge. Although the degree of pathology and magnitude of transcriptional changes are significantly different between TcdA and TcdB, the overall transcriptional responses to TcdA and TcdB are highly correlated (Fig. 2E). Hence, in general, gene expression that is affected by TcdA is also affected by TcdB but to a lesser extent, suggesting broadly similar *in vivo* cellular responses to TcdA and TcdB.

For an initial perspective of which genes are affected, we present genes differentially expressed 2 h after toxin challenge (Table 1). These include several transcription factors (*Atf3*, *Egr1*, and *Jun*) and an mRNA binding protein (*Zfp36*). Consistent with the observed pathology, several of the affected genes at 2 h are related to the regulation of inflammation (*C3*, *Cxcl1*, *Cxcl10*, *Dusp1*, *Egr1*, etc.). Increased expression of *Sprr1a* and *Atf3*, markers of neuronal damage, is interesting with respect to previous findings implicating involvement of the enteric nervous system in the host response (43, 44). *Rhob*, upregulated in our and others' previous *in vitro* studies, is also upregulated in these experiments (26, 45). Manually scanning large lists of differentially expressed genes provides novel and interesting findings yet is impractical when the list includes thousands of genes, as is the case at 6 and 16 h. This manual approach also overlooks groups of genes that are only slightly regulated but in a coordinated fashion. Therefore, we performed bioinformatics analyses to identify other potentially important yet not readily apparent associations that could reflect important functional relationships.

Many statistical tools, termed enrichment methods, can be used to determine if the transcription of predefined sets of genes is significantly altered or enriched; this approach allows for the characterization of cellular processes (instead of individual genes) that are affected. Given our experimental design, we carefully chose two enrichment methods. In our implementation of a competitive enrichment method named CAMERA, which was developed by Wu and Smyth, we test whether the genes in a set are more differ-

TABLE 2 Biological functions and gene sets associated with gene expression changes 2 h after TcdA or TcdB injection[a]

Gene set and function	$Log_{10}(P)$ value[b]	q	Database[c]
TcdA			
Interleukin-1-mediated signaling pathway	5.3	0.003	BP
Cellular response to hydrogen peroxide	5.1	0.003	BP
Positive regulation of fatty acid biosynthetic process	4.0	0.026	BP
Cholesterol metabolic process	3.7	0.042	BP
Hormone activity	4.2	0.021	MF
Innate immunity signaling	3.9	0.047	Reactome
TcdB			
Negative regulation of the Notch signaling pathway	5.7	0.002	BP
Nuclear envelope lumen	3.6	0.045	CC
Genes involved in apoptotic cleavage of cellular proteins	4.0	0.037	Reactome
Membrane trafficking	3.6	0.043	Reactome

[a] Our self-contained enrichment test was run on multiple databases separately, and gene sets with $q < 0.05$ are shown.
[b] The logarithms of the P values from the enrichment test are shown.
[c] The Gene Ontology database is separated into three ontologies: molecular functions (MF), biological processes (BP), and cellular components (CC). Mouse genes were mapped to human orthologs so that the Reactome database could be used.

TABLE 3 Molecular functions associated with gene expression changes 16 h after TcdA injection[a]

Gene set description	$Log_{10}(P)$ value	q
Cell surface binding	3.5	0.102
Rho GTPase binding	3.3	0.102
GTPase activity	3.1	0.107
GTP binding	2.9	0.107
Protein N terminus binding	2.5	0.205
Glutathione transferase activity	2.3	0.205
Steroid binding	2.3	0.205
Carboxylase activity	2.2	0.205
RNA polymerase II core promoter sequence-specific DNA binding	2.2	0.205
Protein complex binding	2.1	0.205
Heme binding	2.1	0.205
Thiolester hydrolase activity	2.1	0.205
Fibronectin binding	2.1	0.205
Cholesterol binding	2.1	0.205
Histone deacetylase activity	2.1	0.205
Triglyceride lipase activity	2.0	0.210
Selenium binding	2.0	0.210
Aromatase activity	2.0	0.210
Beta-tubulin binding	1.9	0.210
Actin binding	1.9	0.210

[a] The top 20 competitively enriched gene sets from the molecular function ontology of the Gene Ontology database are shown.

entially expressed than those outside the set (42). We also developed a self-contained test, inspired by CAMERA, to determine if the average change in gene expression within each gene set is different than zero. Whereas the competitive hypothesis may find a gene set (with several differentially expressed genes) to be insignificant because many genes outside the set are also differentially expressed, the self-contained hypothesis would find the same set to be significant. The self-contained test identified enriched functions for all samples; for TcdA and TcdB samples at 2 h, which have few differentially expressed genes, multiple gene sets are enriched (Table 2). Using the competitive test for TcdA samples, no functions are enriched at 6 h ($q < 0.2$) but several are enriched at 16 h (Table 3). The genes within these groups are presented below.

One of the most striking upregulated sets of genes includes those encoding proteins which bind to GTP or GTPases (Table 3). These expression changes are most evident for TcdA at 16 h, although a similar pattern is observed at earlier time points and with TcdB (Fig. 3A). The expression of interferon-inducible GTPase genes is increasingly affected from 2 to 16 h with either toxin. To a lesser extent, the expression of several small GTPase genes not directly tied to interferons or immune function is also altered. These small GTPases include members of several subfamilies from the Ras protein superfamily. Genes encoding proteins which interact or bind with Rho family proteins were also upregulated. Hence, in addition to the toxins' glucosylation of small GTPases, the *in vivo* transcription of many GTP and GTPase binding proteins with a wide range of functions is clearly altered in response to TcdA and TcdB.

We also found an abundance of differentially expressed genes associated with cell metabolism (Tables 2 and 3). More specifically, many enzymes involved in fatty acid breakdown and beta-oxidation were downregulated. Four other classes of enzymes were also downregulated: cytochrome P450 enzymes, glutathione *S*-transferases, carboxylesterases, and sulfotransferases (Fig. 3B). These genes span several metabolic pathways, yet there is a strong commonality in their substrates, most of which include lipid and fatty acids or related compounds, xenobiotics, or both. In addition to the conspicuous toxin-induced pathology and inflammation, recognition of the altered expression of detoxification enzymes and fatty acid metabolic enzymes introduces an unexplored aspect of the host response to TcdA and TcdB.

Inflammation is a clear pathophysiological manifestation of toxin injection, and many inflammation-associated genes are differentially expressed (Table 1 and Fig. 3C). However, at 6 and 16 h, genes associated with inflammation are not expressed to a greater extent than genes associated with several other functions (Table 3). Competitive enrichment tests did find inflammatory response and chemotaxis among the top six enriched functions for TcdA at 6 h, but the enrichment of these groups is not significant ($q = 0.32$). Given the importance of inflammation in our physiological measurements at 6 and 16 h but no remarkable regulation of only inflammation-associated genes at these times, we further investigated the expression of genes known to be linked with inflammation and related physiological effects.

To identify temporal expression patterns, we clustered genes associated with immune regulation and inflammation according to their change in expression over time (Fig. 3C). Several of these genes are upregulated at 6 h and still at 16 h, which may represent transcription that perpetuates the inflammatory response or has anti-inflammatory effects. For TcdA, expression of five chemokine genes (*Cxcl1*, *Cxcl2*, *Cxcl3*, *Cxcl10*, and *Ccl3*) is strongly upregulated at 6 h (coinciding with increased neutrophil infiltration) but subsides by 16 h. The gene expression of several of these chemokines also correlates with protein expression ($r = 0.67$ for TcdA at 6 h; see Fig. S5 in the supplemental material). Although the 6-h peak in chemokine gene expression does not occur with TcdB, TcdA-induced and TcdB-induced gene expression changes

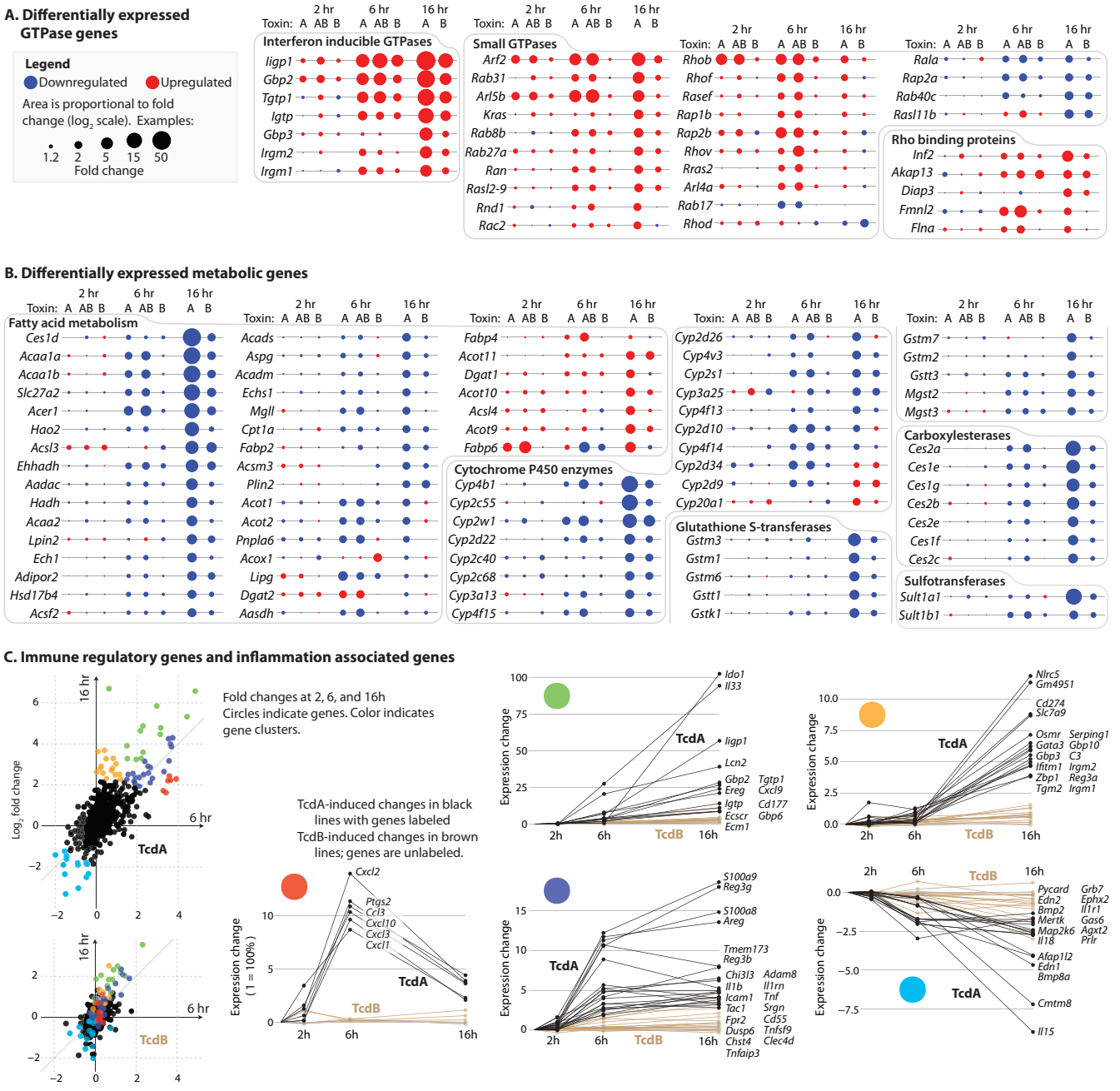

FIG 3 Biological functions associated with gene expression changes. The expression data were generated from the mice depicted in Fig. 2B. (A) The fold changes of differentially expressed GTPase and GTPase-binding genes. Only genes with greater than a 2-fold change in expression are shown. (B) Fold changes as described for panel A but instead showing genes associated with metabolic functions associated with gene expression changes. (C) Expression changes and clustering of genes annotated as being associated with immune regulation or inflammation. Genes were clustered based on expression changes 6 and 16 h after TcdA injection. In the scatterplots, black circles indicate genes with low expression changes; these genes are not included in the line plots.

are correlated for all other inflammatory genes (see Fig. S6). Hence, except for the aforementioned chemokines, TcdA and TcdB similarly regulate inflammation-associated and immune-regulatory genes, although TcdA-induced changes are, on average, two and three times greater at 6 and 16 h, respectively.

CXCL1 and CXCL2 neutralization alters the host response to TcdA cecal injection. To investigate the role of these acutely expressed chemokine genes in response to TcdA challenge, we administered neutralizing antibodies against CXCL2 and the closely related CXCL1. In addition to the high expression of *Cxcl2*, we also chose *Cxcl1* because it is another important primary neutrophil chemoattractant. Anti-CXCL1 and anti-CXCL2 (or corresponding isotypes) were administered by intraperitoneal injection (100 μg/antibody/animal) 16 h prior to TcdA cecal injection. TcdA-induced increases in the serum levels of CXCL1 and CXCL2 are significantly reduced in mice pretreated with anti-CXCL1 and anti-CXCL2, demonstrating that systemic levels were effectively neutralized compared to isotype controls ($P < 0.01$ for CXCL1,

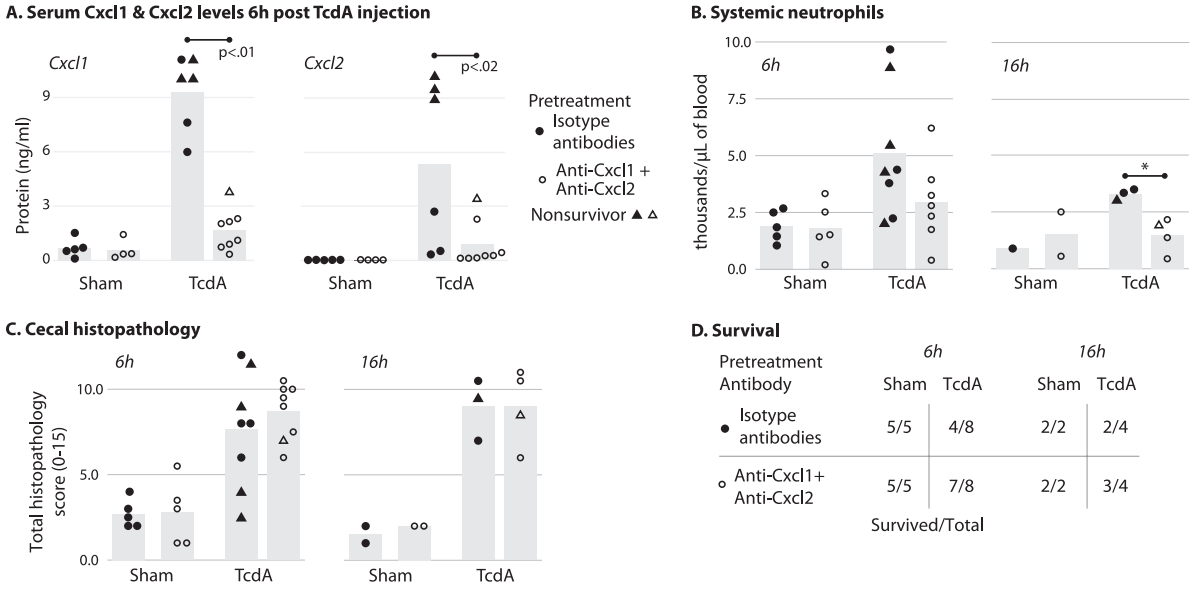

Pretreatment Antibody	6h Sham	6h TcdA	16h Sham	16h TcdA
Isotype antibodies	5/5	4/8	2/2	2/4
Anti-Cxcl1+ Anti-Cxcl2	5/5	7/8	2/2	3/4

FIG 4 Antibody neutralization of CXCL1 and CXCL2. In each panel, the four sample groups are defined by two binary factors: (i) TcdA injection or sham injection and (ii) pretreatment with isotype antibodies or anti-CXCL1 and anti-CXCL2 antibodies. The data in all panels are combined from two independent experiments, one with 24 mice and another with 14 mice (see Table S2 in the supplemental material). Missing values in panels A and B are due to the limited volume of blood that could be drawn from some mice. The data points displayed in the figure were used for each statistical test. Statistical tests are indicated with horizontal lines as described in the legend to Fig. 2. (A) Concentration of CXCL1 and CXCL2 in the sera of mice 6 h after cecal injection of TcdA. (B) Concentration of neutrophils in blood obtained by cardiac puncture. *, $P = 0.057$ by the Mann-Whitney U test. Using this nonparametric, two-sided test with three samples in one group and four in the other, the minimum possible P value is 0.057. $P < 0.02$ by the two-sided t test. (C) Total histopathology score (see Materials and Methods) from cecal tissue sections. (D) Survival of mice after cecal injection. Mice were monitored so that moribund mice were sacrificed and are counted as having not survived (nonsurvivors).

$P < 0.02$ for CXCL2) (Fig. 4A). To test if neutralization of CXCL1 and CXCL2 alters expression of *Cxcl1* and *Cxcl2*, we isolated mRNA from epithelial-layer cells. We found that neutralization does not eliminate the 6-h peak in *Cxcl1* and *Cxcl2* expression caused by TcdA (see Fig. S7 in the supplemental material). In addition, pathology and neutrophil infiltration in the cecum is not affected by administration of anti-CXCL1 and anti-CXCL2 (Fig. 4C; also see Fig. S8). However, 16 h after TcdA injection, systemic neutrophil levels are reduced by neutralization (Fig. 4B). A larger percentage of mice survived after CXCL1 and CXCL2 neutralization, although the experiment was not designed to assess survival and more samples would be necessary to determine statistical significance (Fig. 4D). However, higher serum levels of CXCL1 and CXCL2 correlate with a moribund state, and administration of anti-CXCL1 and anti-CXCL2 reduces those chemokine elevations.

DISCUSSION

This is the first study to characterize the genome-wide transcriptional response to TcdA and TcdB *in vivo*. Additionally, several other parallel measurements were assessed to quantify changes at the cellular and tissue levels. The overall dynamics of the host responses to TcdA include rapid changes in cecal pathology, neutrophil infiltration, and gene expression. Conversely, TcdB elicits a delayed transcriptional response and causes significantly less pathology yet still recruits neutrophils and induces histopathological changes by 16 h. The combined effects of TcdA and TcdB (20 μg/toxin) on histopathology at 2 h and the overall transcriptional response at 2 and 6 h are not additive. However, two of three mice injected with TcdA+B did not survive to our 6-h time point, so we do not rule out potential synergism at later times. For example, Hirota et al., using lower doses (5 μg/toxin), found that TcdA and TcdB may act synergistically 4 h after both toxins are introduced intrarectally (46). As for TcdB alone, several studies have found that TcdB does not damage hamster or mouse intestines, and TcdB does not bind to hamster brush border membranes (16, 18). However, Lyerly et al. showed that when the cecum was bruised before intragastric administration of TcdB, all mice became ill (16). Hence, it is possible that the experimental procedure of cecal injection allows or enhances the TcdB-induced pathology we observe at 16 h. In line with our findings that TcdB has pathological effects, Libby et al. found that 16 of 16 hamsters died within 36 h of cecal injection of 60 μg of TcdB and found that 35 μg of TcdA resulted in epithelial lesions, edema, and neutrophil infiltration (7). We were able to quantify separate aspects of these host responses over time, revealing the relative responses to TcdA and TcdB, individually altered genes and markers of intoxication, and regulated gene sets associated with pathways that function at the intracellular and extracellular levels.

This study builds on our previous analysis of the transcriptional response of a human ileocecal epithelial cell line (HCT8) to TcdA or TcdB (2, 6, and 24 h after toxin treatment). After mapping all orthologous genes, we found that the overall transcriptional response of HCT8 cells is poorly correlated with the responses of the cecal epithelial-layer cells *in vivo* ($r^2 < 0.03$ for all comparisons; see Fig. S9 in the supplemental material). Some of these dissimilarities presumably are due to the different experimental systems and mRNA sources (*in vitro* versus *in vivo* and human versus mouse). Many differences may also represent important responses primarily observed in an *in vivo* experimental

system. For instance, transient expression of chemokines and increased expression of several other cytokines was not observed in HCT8 cells. Also, the altered expression of many metabolic genes did not occur in HCT8 cells. Conversely, cell cycle- and DNA damage-associated gene sets were not enriched *in vivo* as they were with HCT8 cells. Selecting for expression that is similar between the data sets, 10 genes are commonly upregulated (*Rhob*, *Klf2*, *Klf6*, *Jun*, *Dusp1*, *Gdf15*, *Hspa1a*, *Dusp1*, *Bcl2l15*, and *Gpx2*) and a few are commonly downregulated (*Edn1*, *Alpi*, and *Bmp2*) (see Fig. S10). In another high-throughput analysis of the host cell response to TcdA, Zeiser et al. analyzed the changes in the proteome of Caco2 cells 24 h after TcdA exposure (47). By mapping transcripts to proteins, we found that the proteomics data were poorly correlated with transcriptional changes in HCT8 cells and our *in vivo* data ($r^2 < 0.01$ for all comparisons). However, similar to our previous study and the current study, Zeiser et al. did note changes in the amount of many cell cycle-associated proteins and several proteins involved in lipid and cholesterol metabolism.

Aside from the quantitative and temporal differences of the physiological responses, many transcriptional similarities exist between the host response to TcdA and TcdB. For both toxins, the immediate transcriptional response, indicative of initial or acute toxin effects, is represented by altered expression of a small set of genes. By 6 h, the number of differentially expressed genes for both toxins increases ~200-fold, coinciding with changes in pathology, including neutrophil infiltration. TcdA challenge leads to approximately 10-fold more differentially expressed genes at 2, 6, and 16 h; however, there is significant overlap in the genes affected by TcdA and TcdB (Fig. 2). Although TcdA-induced changes were greater in magnitude, correlation coefficients (which are scale invariant) between TcdA and TcdB demonstrate strong overall similarity in gene expression signatures (Fig. 2E). This difference in scale between the toxin responses may result from differences in molecular functions and/or the number, type, and sensitivity of cells affected. Which and how many cells are affected might also originate from the differential abilities of TcdA and TcdB to bind and enter intestinal cells. In line with our results showing that TcdB caused significantly less pathology than TcdA, Rolfe found little to no TcdB adsorption relative to TcdA on hamster brush border membranes (18). The location and transport of toxins within the gut, which is very poorly understood, may also partly explain the extent of pathology in intoxicated mice. After cecal injection of TcdA or TcdB, we did not observe any significant pathology in the colon. Hence, the effects of the toxins which we measured were restricted to the cecum. Nevertheless, other systemic effects emanating from local insult may contribute to overall pathology. Multiple animal studies have observed increased mucosal permeability after TcdA intoxication, and Steele et al. demonstrated systemic dissemination of both TcdA and TcdB during severe infection in mice and piglets (29). Despite the various explanations for the lesser effects we observe with TcdB, a change in transcription after injection of TcdB is distinct even at 2 and 6 h, when changes in histopathology and many other variables are not apparent. Furthermore, this transcriptional response is highly correlated with the response to TcdA. Hence, the transcriptional analysis reveals that overall intracellular responses of epithelial-layer cells to TcdA and TcdB are largely similar, although the magnitudes of the gross observed pathologies may differ.

Beyond piecemeal identification of genes with altered expression, the transcriptional data as a whole reflects the cellular responses to underlying molecular interactions. Our analyses identified the upregulation of several genes encoding Rho binding proteins and small GTPases that are known to be affected by TcdA and TcdB. We also identified strong upregulation of many interferon-inducible GTPases. These interferon-inducible GTPases have been implicated in several mechanisms of cell-autonomous immunity, such as inflammasome activation, recognition of pathogens in vacuoles, assembly of defense complexes, and autophagy (48). Although the transcription of interferon genes is unaltered in the epithelial-layer cells we isolated, the GTPase upregulation suggests the functional presence of interferons. Consistent with this, Ishida et al. found increased transcription of IFN-γ in whole tissue and increased production of IFN-γ by infiltrating neutrophils after injection of TcdA into ligated ileal loops of mice (33). In the same analysis, beta-tubulin binding and histone deacetylase activity were also enriched. Although the relevance of these associations may seem unclear at first, Nam et al. have recently shown that inhibition of histone deacetylase 6 blocks TcdA-induced tubulin acetylation and subsequent mucosal damage (49). Hence, our analysis corroborates previous data and suggests that our transcriptional data reflect other functions that are affected in parallel with or prior to transcription. For example, a novel set of toxin-induced genes identified in our analysis includes several metabolic genes. At 2 h, multiple genes associated with cholesterol and steroid synthesis (specifically the mevalonate pathway) are slightly upregulated, whereas at 6 and 16 h, genes associated with fatty acid metabolism and detoxification of xenobiotics are downregulated. The expression of several of these genes is known to be controlled directly or indirectly by nuclear receptors. In light of the finding that gp96 (a paralogue to heat shock protein 90 [Hsp90]) serves as a receptor for TcdA *in vitro*, these transcriptional changes may also result from Hsp90 interactions (e.g., Hsp90 proteins bind xenobiotic response elements and steroid hormone receptors) (24).

In addition to the intracellular effects described above, several genes previously associated with toxin-mediated pathophysiology are altered. For instance, our self-contained enrichment test identified the interleukin-1 (IL-1)-mediated signaling pathway as the most enriched gene set 2 h after TcdA injection. More specifically, TcdA increases proinflammatory *Il1b* expression by 80% at 2 h and then over 500% at 16 h; TcdB causes no such change. In addition to *Il1b*, concomitant increases in the IL-1 receptor antagonist, *Il1rn*, suggest a natural feedback mechanism. These findings are in line with a previous study demonstrating that recombinant IL1RN pretreatment attenuated TcdA+B-induced inflammation (50). Expression of *Il33*, an IL-1 family cytokine involved in mucosal signaling, also dramatically increases in response to TcdA (28- and 95-fold at 6 and 16 h, respectively). Similarly, in mice infected with *C. difficile* (VPI 10463), intestinal levels of IL-33 increase at the peak of infection (data not shown), suggesting that this cytokine is responsive in part to toxin effects. In another study, Hirota et al. measured cytokine levels in colonic tissue lysates 4 h after intrarectal instillation of TcdA+B. The data published by Hirota et al. are correlated with our measured cecal, epithelial-layer gene expression ($r = 0.5$ for TcdA+B at 6 h) and intracellular protein expression ($r = 0.36$ for TcdA at 6 h) (see Fig. S5 in the supplemental material). Six hours after cecal injection of TcdA, serum cytokine concentrations correlate even more strongly with Hirota et al.'s data ($r = 0.68$). Hence, our data from cecal cells and serum after cecal injection of TcdA and/or TcdB are

in agreement with findings from colonic tissue after intrarectal instillation of TcdA+B. Additionally, our data show the expression changes of many other genes over a 16-h time course for each toxin individually.

Although the expression and/or release of chemokines and cytokines are known responses to *C. difficile* toxins, the full profile of the transcription of cytokines in response to toxins has not been investigated. Previously, the role of many chemokines and proinflammatory mediators in TcdA-induced enteritis has been studied individually with ileal loops or *in vitro* (27). For example, Morteau et al. found increased *Ccl3* and *Ccl5* transcription in whole tissue 1 h after TcdA injection and showed that *Ccl3* knockout mice were less susceptible to TcdA (30). Castagliuolo et al. identified increased expression of *Cxcl2* in rat epithelial cells after injection of TcdA into ligated ileal loops (34). Our results identify additional chemokines which are transiently expressed and provide insight into the response of the epithelial layer over a time course covering the development of toxin-mediated pathogenesis. Additionally, our data include the expression of all cytokines in response to TcdA and TcdB separately and in combination. We found that overall cytokine expression in response to TcdA and TcdB is correlated, yet TcdA-induced changes are more pronounced. However, TcdB does not increase the expression of several inflammation-associated chemokines as TcdA does. This difference between toxins is particularly interesting in light of the fact that TcdB cecal injection causes less tissue damage and inflammation than injection of TcdA. Our data also show that the chemokine expression in response to TcdA is transient, yet many other cytokines continue to be expressed even after chemokine expression returns to basal levels. The early chemokine expression may be involved in the acute toxin effects. However, since *C. difficile* infections typically last several days, the continued expression of several other cytokines is an unexplored and potentially interesting area of research.

In order to characterize the timing and the effects of the acute response after toxin exposure, we investigated the early effects of CXCL1 and CXCL2 in the same cecal injection system. The increased expression of chemokine genes involved in neutrophil recruitment (e.g., *Cxcl1* and *Cxcl2*) was coincident with neutrophil infiltration. Local epithelial damage and neutrophil infiltration were not attenuated by neutralization of CXCL1 and CXCL2. Similar findings in pathology between neutralizing antibodies and isotype controls could be due to insufficient levels of antibody near the site of toxin injection or the method of antibody administration. In another neutralization study, Castagliuolo et al. injected anti-CXCL2 intravenously into fasted rats 15 min prior to injection of TcdA into ileal loops; this neutralization attenuated TcdA-induced fluid secretion, mucosal permeability, and MPO activity (34). Other ileal loop experiments with TcdA have revealed that pathology and neutrophil infiltration become evident 1 to 3 h after intoxication (33, 34). Hence, it is unlikely that the effects we measured in this study would have been discernible prior to our earliest 2-h time point. On the other hand, few studies have examined the host responses after the initial acute response; most have focused on responses within the first 6 h (30–33, 35, 36, 51). Our latest time point, 16 h, did reveal attenuation of the TcdA-induced increase in systemic neutrophils for anti-CXCL1- and anti-CXCL2-treated animals. Moreover, serum levels of CXCL1 and CXCL2 were predictors for survival. This result also suggests that surviving mice are poor responders in terms of *Cxcl1* and *Cxcl2* expression and production. Related to this, a recent study by El Feghaly et al. showed that inflammatory markers in stool, not the number of *C. difficile* CFU, correlated with clinical outcomes (52). In a hamster infection model, Steele et al. showed that serum levels of CXCL1, IL-6, tumor necrosis factor α, and IL-1β are increased in cases of severe, systemic infection (29). Our results demonstrating that high CXCL1 and CXCL2 correlate with mortality are supportive of these infection studies and suggest that the release of these and perhaps other inflammatory markers in serum is primarily toxin mediated. Thus, our experiments with anti-CXCL1 and anti-CXCL2 emphasize the importance of the locale of toxin effects and chemokine expression systemically and/or throughout the intestine.

The multilevel measurements and our analysis have revealed important aspects of the relative host responses to TcdA versus TcdB intoxication, novel changes in transcription underlying observed physiological changes, and many aspects of the early time course and dynamics of the host response near the site of injection and in circulating blood. These extensive data and experimental framework also provide a basis for comparisons and future investigations with mutant toxins and mutant mouse strains. Furthermore, these data may be used to identify diagnostic markers or novel targets to attenuate host responses to TcdA and TcdB.

ACKNOWLEDGMENTS

We thank David Bolick for his technical expertise, David Lyerly at TECHLAB, Inc., for providing purified TcdA and TcdB, and Stephen Becker and Eric Houpt for providing immortalized mouse epithelial cells.

We have no conflicts of interest to disclose.

This work was supported by the National Institute of Allergy and Infectious Diseases Regional Center of Excellence program through the Mid-Atlantic Regional Center of Excellence in Biodefense and Emerging Infections (2 5U54 AI057168). K.M.D. is a trainee on the Infectious Diseases Training Grant to the University of Virginia Division of Infectious Diseases and International Health (5T32 AI007046).

REFERENCES

1. **Lucado J, Gould C, Elixhauser A.** 2012. Clostridium difficile infections (CDI) in hospital stays, 2009. HCUP statistical brief 124. Agency for Healthcare Research and Quality, Rockville, MD.
2. **Ghantoji SS, Sail K, Lairson DR, DuPont HL, Garey KW.** 2010. Economic healthcare costs of Clostridium difficile infection: a systematic review. J. Hosp. Infect. **74:**309–318.
3. **McGlone SM, Bailey RR, Zimmer SM, Popovich MJ, Tian Y, Ufberg P, Muder RR, Lee BY.** 2012. The economic burden of Clostridium difficile. Clin. Microbiol. Infect. **18:**282–289.
4. **Dubberke ER, Olsen MA.** 2012. Burden of Clostridium difficile on the healthcare system. Clin. Infect. Dis. **55**(Suppl. 2):S88–S92.
5. **Lyras D, O'Connor JR, Howarth PM, Sambol SP, Carter GP, Phumoonna T, Poon R, Adams V, Vedantam G, Johnson S, Gerding DN, Rood JI.** 2009. Toxin B is essential for virulence of Clostridium difficile. Nature **458:**1176–1179.
6. **Kuehne SA, Cartman ST, Heap JT, Kelly ML, Cockayne A, Minton NP.** 2010. The role of toxin A and toxin B in Clostridium difficile infection. Nature **467:**711–713.
7. **Libby JM, Jortner BS, Wilkins TD.** 1982. Effects of the two toxins of Clostridium difficile in antibiotic-associated cecitis in hamsters. Infect. Immun. **36:**822–829.
8. **Von Eichel-Streiber C, Laufenberg-Feldmann R, Sartingen S, Schulze J, Sauerborn M.** 1992. Comparative sequence analysis of the Clostridium difficile toxins A and B. Mol. Gen. Genet. **233:**260–268.
9. **Chaves-Olarte E, Weidmann M, Eichel-Streiber C, Thelestam M.** 1997. Toxins A and B from Clostridium difficile differ with respect to enzymatic potencies, cellular substrate specificities, and surface binding to cultured cells. J. Clin. Investig. **100:**1734–1741.

10. **Taylor NS, Thorne GM, Bartlett JG.** 1981. Comparison of two toxins produced by Clostridium difficile. Infect. Immun. **34:**1036–1043.
11. **Jank T, Aktories K.** 2008. Structure and mode of action of clostridial glucosylating toxins: the ABCD model. Trends Microbiol. **16:**222–229.
12. **Carter GP, Rood JI, Lyras D.** 2012. The role of toxin A and toxin B in the virulence of Clostridium difficile. Trends Microbiol. **20:**21–29.
13. **Drudy D, Fanning S, Kyne L.** 2007. Toxin A-negative, toxin B-positive Clostridium difficile. Int. J. Infect. Dis. **11:**5–10.
14. **Small JD.** 1968. Fatal enterocolitis in hamsters given lincomycin hydrochloride. Lab. Anim. Care **18:**411–420.
15. **Bartlett JG, Onderdonk AB, Cisneros RL, Kasper DL.** 1977. Clindamycin-associated colitis due to a toxin-producing species of Clostridium in hamsters. J. Infect. Dis. **136:**701–705.
16. **Lyerly DM, Saum KE, MacDonald DK, Wilkins TD.** 1985. Effects of Clostridium difficile toxins given intragastrically to animals. Infect. Immun. **47:**349–352.
17. **Savidge TC, Pan WH, Newman P, O'Brien M, Anton PM, Pothoulakis C.** 2003. Clostridium difficile toxin B is an inflammatory enterotoxin in human intestine. Gastroenterology **125:**413–420.
18. **Rolfe RD.** 1991. Binding kinetics of Clostridium difficile toxins A and B to intestinal brush border membranes from infant and adult hamsters. Infect. Immun. **59:**1223–1230.
19. **Krivan HC, Clark GF, Smith DF, Wilkins TD.** 1986. Cell surface binding site for Clostridium difficile enterotoxin: evidence for a glycoconjugate containing the sequence Gal alpha 1-3Gal beta 1-4GlcNAc. Infect. Immun. **53:**573–581.
20. **Tucker KD, Wilkins TD.** 1991. Toxin A of Clostridium difficile binds to the human carbohydrate antigens I, X, and Y. Infect. Immun. **59:**73–78.
21. **Rolfe RD, Song W.** 1995. Immunoglobulin and non-immunoglobulin components of human milk inhibit Clostridium difficile toxin A-receptor binding. J. Med. Microbiol. **42:**10–19.
22. **Pothoulakis C, Gilbert RJ, Cladaras C, Castagliuolo I, Semenza G, Hitti Y, Montcrief JS, Linevsky J, Kelly CP, Nikulasson S, Desai HP, Wilkins TD, LaMont JT.** 1996. Rabbit sucrase-isomaltase contains a functional intestinal receptor for Clostridium difficile toxin A. J. Clin. Investig. **98:**641–649.
23. **Pothoulakis C, Galili U, Castagliuolo I, Kelly CP, Nikulasson S, Dudeja PK, Brasitus TA, LaMont JT.** 1996. A human antibody binds to alpha-galactose receptors and mimics the effects of Clostridium difficile toxin A in rat colon. Gastroenterology **110:**1704–1712.
24. **Na X, Kim H, Moyer MP, Pothoulakis C, LaMont JT.** 2008. gp96 is a human colonocyte plasma membrane binding protein for Clostridium difficile toxin A. Infect. Immun. **76:**2862–2871.
25. **El-Hawiet A, Kitova EN, Kitov PI, Eugenio L, Ng KK, Mulvey GL, Dingle TC, Szpacenko A, Armstrong GD, Klassen JS.** 2011. Binding of Clostridium difficile toxins to human milk oligosaccharides. Glycobiology **21:**1217–1227.
26. **D'Auria KM, Donato GM, Gray MC, Kolling GL, Warren CA, Cave LM, Solga MD, Lannigan JA, Papin JA, Hewlett EL.** 2012. Systems analysis of the transcriptional response of human ileocecal epithelial cells to Clostridium difficile toxins and effects on cell cycle control. BMC Syst. Biol. **6:**2. doi:10.1186/1752-0509-6-2.
27. **Sun X, Savidge T, Feng H.** 2010. The enterotoxicity of Clostridium difficile toxins. Toxins (Basel) **2:**1848–1880.
28. **Madan R, Petrie WA, Jr.** 2012. Immune responses to Clostridium difficile infection. Trends Mol. Med. **18:**658–666.
29. **Steele J, Chen K, Sun X, Zhang Y, Wang H, Tzipori S, Feng H.** 2012. Systemic dissemination of Clostridium difficile toxins A and B is associated with severe, fatal disease in animal models. J. Infect. Dis. **205:**384–391.
30. **Morteau O, Castagliuolo I, Mykoniatis A, Zacks J, Wlk M, Lu B, Pothoulakis C, Gerard NP, Gerard C.** 2002. Genetic deficiency in the chemokine receptor CCR1 protects against acute Clostridium difficile toxin A enteritis in mice. Gastroenterology **122:**725–733.
31. **Kelly CP, Becker S, Linevsky JK, Joshi MA, O'Keane JC, Dickey BF, LaMont JT, Pothoulakis C.** 1994. Neutrophil recruitment in Clostridium difficile toxin A enteritis in the rabbit. J. Clin. Investig. **93:**1257–1265.
32. **Kokkotou E, Espinoza DO, Torres D, Karagiannides I, Kosteletos S, Savidge T, O'Brien M, Pothoulakis C.** 2009. Melanin-concentrating hormone (MCH) modulates C difficile toxin A-mediated enteritis in mice. Gut **58:**34–40.
33. **Ishida Y, Maegawa T, Kondo T, Kimura A, Iwakura Y, Nakamura S, Mukaida N.** 2004. Essential involvement of IFN-gamma in Clostridium difficile toxin A-induced enteritis. J. Immunol. **172:**3018–3025.
34. **Castagliuolo I, Keates AC, Wang CC, Pasha A, Valenick L, Kelly CP, Nikulasson ST, LaMont JT, Pothoulakis C.** 1998. Clostridium difficile toxin A stimulates macrophage-inflammatory protein-2 production in rat intestinal epithelial cells. J. Immunol. **160:**6039–6045.
35. **Warny M, Keates AC, Keates S, Castagliuolo I, Zacks JK, Aboudola S, Qamar A, Pothoulakis C, LaMont JT, Kelly CP.** 2000. p38 MAP kinase activation by Clostridium difficile toxin A mediates monocyte necrosis, IL-8 production, and enteritis. J. Clin. Investig. **105:**1147–1156.
36. **Alcantara CS, Jin XH, Brito GA, Carneiro-Filho BA, Barrett LJ, Carey RM, Guerrant RL.** 2005. Angiotensin II subtype 1 receptor blockade inhibits Clostridium difficile toxin A-induced intestinal secretion in a rabbit model. J. Infect. Dis. **191:**2090–2096.
37. **Becker SM, Cho K-N, Guo X, Fendig K, Oosman MN, Whitehead R, Cohn SM, Houpt ER.** 2010. Epithelial cell apoptosis facilitates Entamoeba histolytica infection in the gut. Am. J. Pathol. **176:**1316–1322.
38. **Pawlowski SW, Calabrese G, Kolling GL, Freire R, AlcantaraWarren C, Liu B, Sartor RB, Guerrant RL.** 2010. Murine model of Clostridium difficile infection with aged gnotobiotic C57BL/6 mice and a BI/NAP1 strain. J. Infect. Dis. **202:**1708–1712.
39. **Albert EJ, Duplisea J, Dawicki W, Haidl ID, Marshall JS.** 2011. Tissue eosinophilia in a mouse model of colitis is highly dependent on TLR2 and independent of mast cells. Am. J. Pathol. **178:**150–160.
40. **Irizarry RA, Hobbs B, Collin F, Beazer-Barclay YD, Antonellis KJ, Scherf U, Speed TP.** 2003. Exploration, normalization, and summaries of high density oligonucleotide array probe level data. Biostatistics **4:**249–264.
41. **Baldi P, Long AD.** 2001. A Bayesian framework for the analysis of microarray expression data: regularized t-test and statistical inferences of gene changes. Bioinformatics **17:**509–519.
42. **Wu D, Smyth GK.** 2012. Camera: a competitive gene set test accounting for inter-gene correlation. Nucleic Acids Res. **40:**e133.
43. **Starkey ML, Davies M, Yip PK, Carter LM, Wong DJ, McMahon SB, Bradbury EJ.** 2009. Expression of the regeneration-associated protein SPRR1A in primary sensory neurons and spinal cord of the adult mouse following peripheral and central injury. J. Comp. Neurol. **513:**51–68.
44. **Linhoff MW, Lauren J, Cassidy RM, Dobie FA, Takahashi H, Nygaard HB, Airaksinen MS, Strittmatter SM, Craig AM.** 2009. An unbiased expression screen for synaptogenic proteins identifies the LRRTM protein family as synaptic organizers. Neuron **61:**734–749.
45. **Gerhard R, Tatge H, Genth H, Thum T, Borlak J, Fritz G, Just I.** 2005. Clostridium difficile toxin A induces expression of the stress-induced early gene product RhoB. J. Biol. Chem. **280:**1499–1505.
46. **Hirota SA, Iablokov V, Tulk SE, Schenck LP, Becker H, Nguyen J, Al Bashir S, Dingle TC, Laing A, Liu J, Li Y, Bolstad J, Mulvey GL, Armstrong GD, MacNaughton WK, Muruve DA, MacDonald JA, Beck PL.** 2012. Intrarectal instillation of Clostridium difficile toxin A triggers colonic inflammation and tissue damage: development of a novel and efficient mouse model of Clostridium difficile toxin exposure. Infect. Immun. **80:**4474–4484.
47. **Zeiser J, Gerhard R, Just I, Pich A.** 2013. Substrate specificity of clostridial glucosylating toxins and their function on colonocytes analyzed by proteomics techniques. J. Proteome Res. [Epub ahead of print.] doi:10.1021/pr300973q.
48. **Kim B-H, Shenoy AR, Kumar P, Bradfield CJ, Macmicking JD.** 2012. IFN-inducible GTPases in host cell defense. Cell Host Microbe **12:**432–444.
49. **Nam HJ, Kang JK, Kim SK, Ahn KJ, Seok H, Park SJ, Chang JS, Pothoulakis C, Lamont JT, Kim H.** 2010. Clostridium difficile toxin A decreases acetylation of tubulin, leading to microtubule depolymerization through activation of histone deacetylase 6, and this mediates acute inflammation. J. Biol. Chem. **285:**32888–32896.
50. **Ng J, Hirota SA, Gross O, Li Y, Ulke-Lemee A, Potentier MS, Schenck LP, Vilaysane A, Seamone ME, Feng H, Armstrong GD, Tschopp J, Macdonald JA, Muruve DA, Beck PL.** 2010. Clostridium difficile toxin-induced inflammation and intestinal injury are mediated by the inflammasome. Gastroenterology **139:**542–552.
51. **Castagliuolo I, LaMont JT, Letourneau R, Kelly C, O'Keane JC, Jaffer A, Theoharides TC, Pothoulakis C.** 1994. Neuronal involvement in the intestinal effects of Clostridium difficile toxin A and Vibrio cholerae enterotoxin in rat ileum. Gastroenterology **107:**657–665.
52. **El Feghaly RE, Stauber JL, Deych E, Gonzalez C, Phillip I, Haslam DB, Louis S, Ave E, States U.** 2013. Markers of intestinal inflammation, not bacterial burden, correlate with clinical outcomes in Clostridium difficile infection. Clin. Infect. Dis. **56:**1713–1721.